



A Comparative Study on the Removal of Cr(VI) using Fire Clay-TiO₂ Nanocomposite and Fire Clay

A. Rathinavelu¹, V. Venkateswaran^{2*}

^{1*}Department of Chemistry, Erode Arts and Science College (Autonomous), Erode, TN, India.

^{2*}Principal, Sree Saraswathi Thyagaraja College (Autonomous), Pollachi, TN, India.

Received:12.12.2014 Accepted:25.01.2015

Abstract

The present study was aimed at investigating the adsorption behaviour of Cr(VI) ions onto fire clay -TiO₂ nanocomposite (NC) and fire clay (FC). The effect of several parameters such as adsorbent dose, contact time, initial concentration, p^H & temperature has been studied. The adsorption followed pseudo second order, Elovich kinetic models. Intraparticle diffusion model has also been attempted. The adsorption of Cr(VI) was found to be maximum in the p^H range 8-11. Adsorption on both clay and nanocomposite obey Langmuir and Freundlich models. The thermodynamic parameters ΔG° , ΔH° , ΔS° have also been evaluated. Adsorptions on both clay and nanocomposite were found to be endothermic and chemisorptive in nature. Chromium removal was better with nanocomposite than with clay.

Keywords: Adsorption isotherm; Fire clay; Fire clay-TiO₂ nanocomposite; Heavy metal.

1. INTRODUCTION

The presence of heavy metals such as Cr(VI) in aqueous streams, arising from the discharge of untreated metal containing effluents into water bodies, is one of the most important environmental issues. Adsorption is one of the technique effectively used for the removal of Cr(VI) from wastewaters (Babu and Gupta, 2005). Several low cost adsorbents from cheaper and readily available materials (Parimaladevi and Venkateswaran, 2011) have been identified for the removal of contaminating materials. Materials such as leaf mould, sugar beet pulp, bagasse, maize cob, biogas residual slurry, Fe(III) / Cr(III) hydroxide have been used for the removal of Cr(VI) from aqueous solutions (Pradhan *et al.* 1999; Das *et al.* 2000; Sarin and Pant, 2005; Singh *et al.* 2005). Studies using clays in their natural form and polymers as adsorbents for removal of heavy metals are also available (Veera *et al.* 2003; Abolino *et al.* 2003). Fire clay and fire clay-TiO₂ (NC) have been used for the removal of basic dyes (Venkateswaran and Priya, 2012). Hence in this study it is proposed to prepare fire clay-TiO₂ nanocomposite, characterize it and evaluate its efficiency in removing hexavalent chromium. Similar studies will be carried out using fire clay in natural form so as to compare their relative adsorption capacities.

2. MATERIALS & METHODS

Fire clay (3 g) was allowed to swell in 15 mL of water-free alcohol and stirred for 2 hrs at 25 °C to get a uniform suspension. At the same time, the titanium dioxide (3 g) was dispersed into water-free alcohol (15 mL). Then the diluted titanium dioxide was slowly added into the suspension of fire clay and stirred for a further 5 hrs at 25 °C. Finally, 5ml alcohol mixed with 0.2 mL deionized water was slowly added. The stirring was continued for another 5 hrs at 25 °C and the resulting suspension kept overnight in a vacuum oven for 6 hrs at 80 °C.

Absorbate solution

A stock solution of Cr(VI) was prepared by dissolving 5.658 g of K₂Cr₂O₇ (99.9%) in 1000 mL of doubly distilled water.

Characterization of adsorbent

Physico-chemical characteristics of the adsorbents were studied as per the standard testing methods. The XRD pattern of pure fire clay fig.1 and that of fire clay-TiO₂ nanocomposite fig. 2 show characteristics peaks at 28° and 30° which confirm the presence of fire clay-TiO₂ phase in the nanocomposite. The surface morphology of the adsorbent was visualized via scanning electron microscopy (SEM) fig. 3 & 4. The diameter of the composite range was 50 µm.

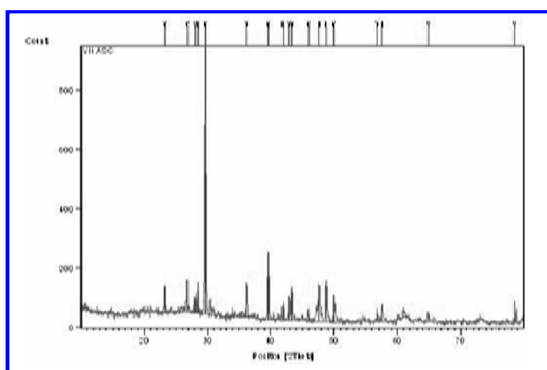


Fig. 1: XRD Analysis of fire clay

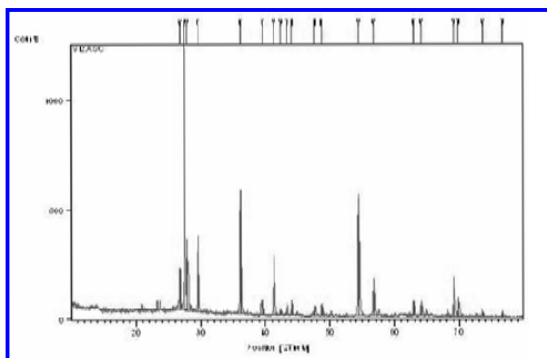


Fig. 2: XRD Analysis of Stishovite-TiO₂ nanocomposites

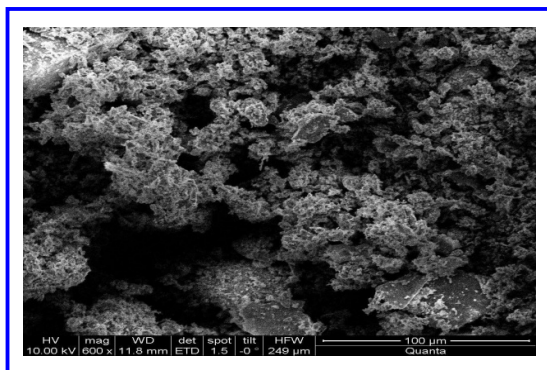


Fig. 3: SEM of pure fire clay

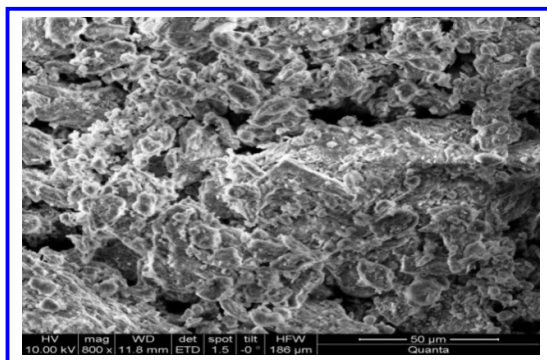


Fig. 4: SEM of pure fire clay-TiO₂ composite

Batch adsorption experiments

Batch adsorption experiments were conducted by agitating the flasks for a predetermined time intervals in a thermostat attached with a shaker at a desired temperature. Adsorption isotherm study was carried out with different initial concentrations of Cr(VI) ranging from 10 to 40 mg/L while maintaining the adsorbent dosage at 0.1 g. The effect of contact time and p^H was studied with Cr(VI) concentration of 10-40 mg/L and an adsorbent dosage of 0.1 g. The solution p^H was adjusted in the range of 5-11 by using dilute hydrochloric acid and sodium hydroxide solutions. Experiments were carried out by varying the adsorbent amount from 0.1 to 1.0 g with Cr(VI) concentration ranging from 10 to 40 mg/L. The concentration of free chromium (VI) ions in the effluent was determined spectrophotometrically by developing a purple-violet color using 1,5-diphenyl carbazide as complexing agent in acidic solution.

3. RESULT & DISCUSSION

Effect of adsorbent dose

The effect of adsorbent dose on Cr(VI) removal was studied by keeping all other experimental conditions constant except that of adsorption dose. The results showed that with increase in adsorbent concentration there is a decrease in the amount adsorbed per unit mass of the adsorbent for both clay and nanocomposite fig. 5 & 6. This may be basically due to adsorption sites remaining unsaturated during the adsorption process.

Effect of contact time and initial metal concentration

The effect of contact time and different initial concentrations has been studied using both clay and nanocomposite. It is observed that in both cases the percentage removal of Cr(VI) ions increase with increase in metal ion concentration (fig. 7, 8) attains saturation in 50 to 135 min with nanocomposite and 60 to 150 min with clay. The removal rate by adsorption is rapid initially, gradually decreases with time and finally attains equilibrium is rapid initially.

Effect of p^H

Adsorption of Cr(VI) was studied at various p^H values and results are depicted in fig. 9 & 10. The initial p^H of solution was varied from 5 to 11 with the

adsorbate concentration varying from 10-40 mg/L maintaining the adsorbent dose at 0.1 g and the contact time as 2 hrs for both clay and nanocomposite.

From fig. 9 & 10 it is clear that chromium adsorption efficiency is highest at p^H 8-11 with nanocomposite and at 7-10 with clay. p^H_{zpc} for the nanocomposite and clay was determined as 8.0.

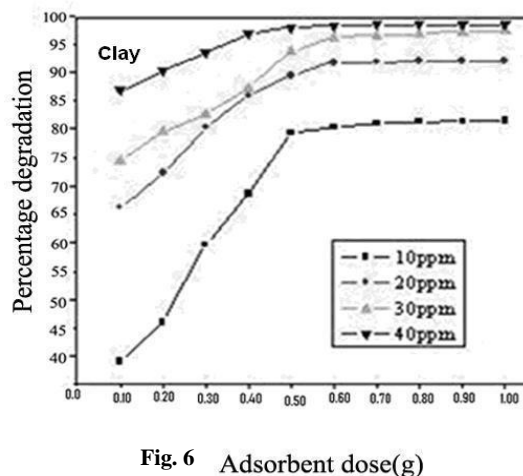
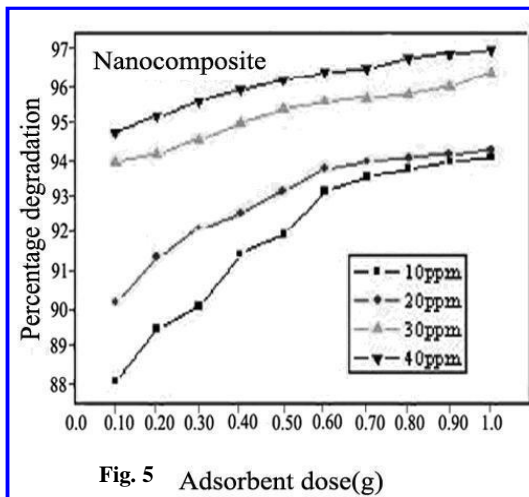


Fig. 5 & Fig. 6

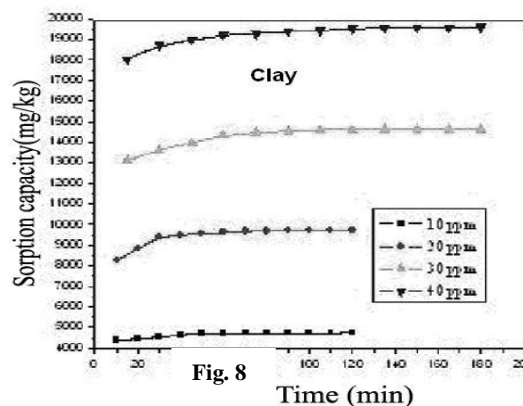
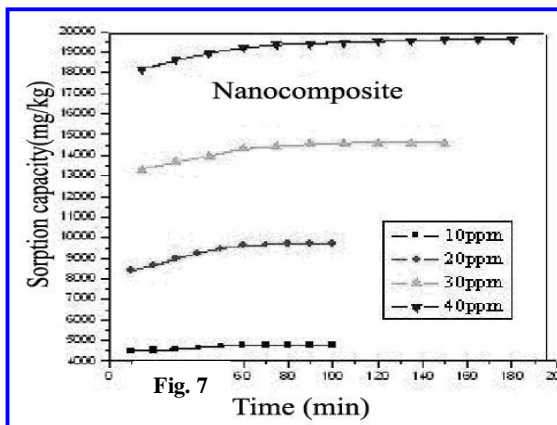


Fig. 7 & Fig. 8: Effect of contact time and initial metal concentration

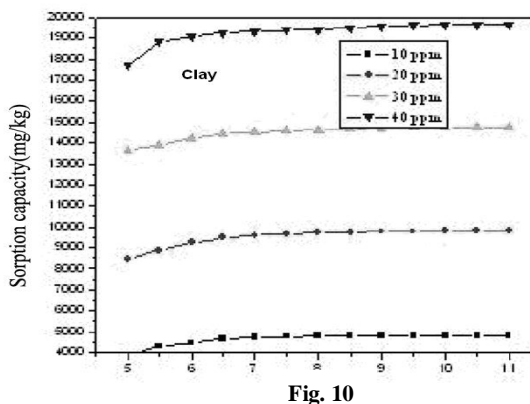
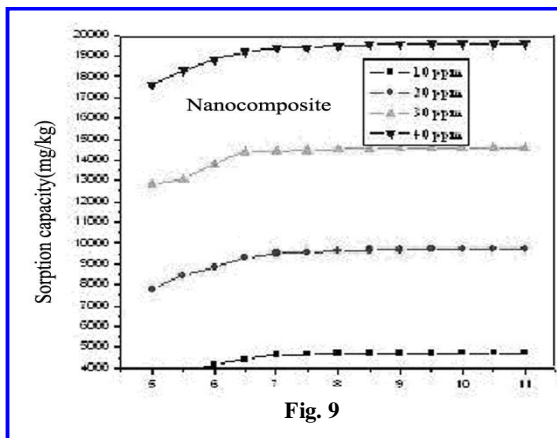


Fig. 9 & Fig. 10: Effect of p^H

Effect of temperature

Effect of temperature on adsorption of Cr(VI) ion was studied at different temperatures viz., 303K, 307K, 311K, 315K and the results are shown in fig. 11 & 12. It is observed that adsorption of chromium ions increases (Koby *et al.* 2000) with increasing temperature showing the process to be endothermic with both adsorbents.

4. ADSORPTION ISOTHERM

4.1 Langmuir adsorption isotherm

The Langmuir isotherm model commonly used for the adsorption of a solute from a aqueous solution (Langmuir, 1916) in its linear form can be represented as

$$C_e / q_e = i/bq_0 + C_e / q_0 \quad (1)$$

Where C_e is the equilibrium concentration of the adsorbate (mg/L), q_e is the amount of metal adsorbed per unit mass of adsorbent (mg/L) and q_0 and 'b' are Langmuir constants related to adsorption capacity and rate of adsorption respectively. As required by equation (1), plotting C_e/q_e against C_e gave a straight line, indicating that the adsorption of heavy metal on both clay and nanocomposite follow the Langmuir isotherm fig. 13 & 14. The Langmuir constants 'b' and q_0 were evaluated from the slope and

intercept of the graph. The essential characteristics of the Langmuir isotherm can be expressed in terms of a dimensionless equilibrium parameter R_L which is defined by,

$$R_L = 1/(1 + bC_0) \quad (2)$$

Where, C_0 is the initial solute concentration, 'b' the Langmuir adsorption constant (L/mg). R_L value less than one indicates favourable adsorption (Norrozi *et al.* 2007). The R_L values shown in table 1 (all <1) confirm that the adsorption of Cr(VI) follow Langmuir isotherm.

4.2 Freundlich model

The Freundlich isotherm, in its logarithmic form can be represented as

$$\log q_e = \log K_f + 1/n \log C_e \quad (3)$$

Where K_f and $1/n$ are Freundlich constants related to adsorption capacity and adsorption intensity of the sorbent respectively. q_e is the amount adsorbed at equilibrium (mg/g); C_e is the equilibrium concentration of the adsorbate. The plot of $\log q_e$ versus $\log C_e$ gave straight lines with good regression coefficients indicating that the adsorption of heavy metal follow the Freundlich isotherm fig. 15 & 16. The values of K_f and $1/n$ calculated from the intercept and slope respectively are recorded in table 2.

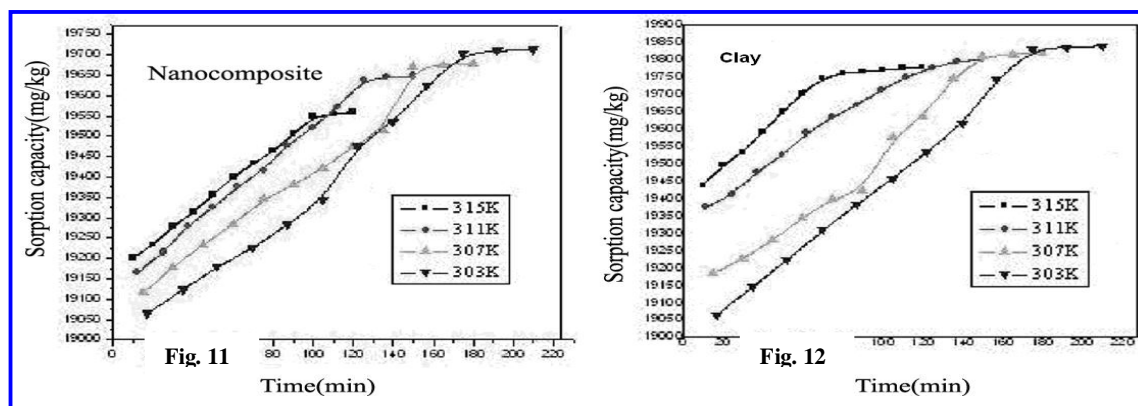


Fig. 11 & Fig. 12: Effect of Temperature

Table 1. The values of Langmuir constant Q^0 and b in addition to R_L

Conc. metal (mg/L)	Fire clay – TiO ₂ nanocomposite				Fire clay			
	R_L	b	Q^0 mg/g	R^2	R_L	B	Q^0 mg/g	R^2
20	0.4789	0.0544	4.2900	0.9946	0.9731	0.0138	136.98	0.9960
40	0.3148				0.6443			
60	0.2345				0.5470			
80	0.1868				0.4752			
100	0.1552				0.4201			
120	0.1328				0.3765			

Table 2. The values of Freundlich constant K_f and n

Adsorbent	K_f (L/mg)	n (mg/g)	R^2
Fire clay-TiO ₂ nanocomposite	22.90	0.146	0.9965
Fire clay	0.057	2.842	0.9950

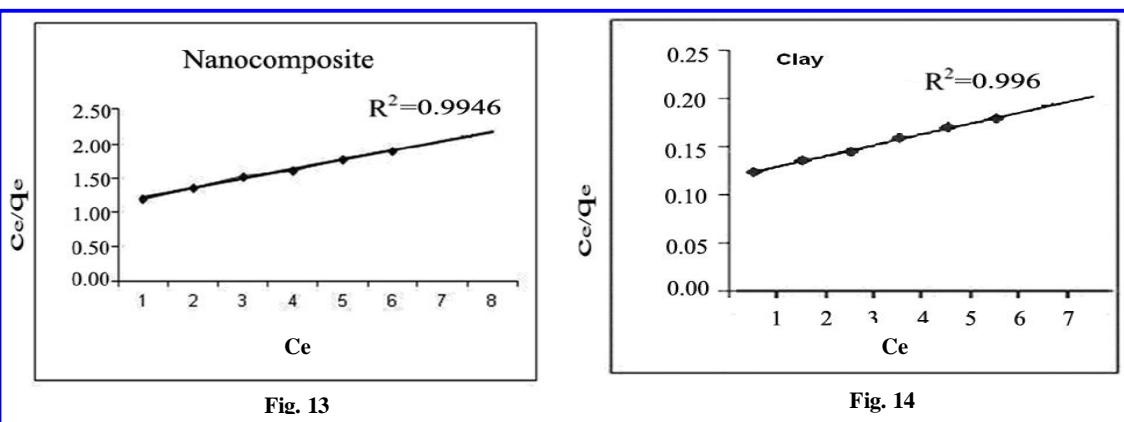


Fig. 13 & Fig. 14: Langmuir isotherm

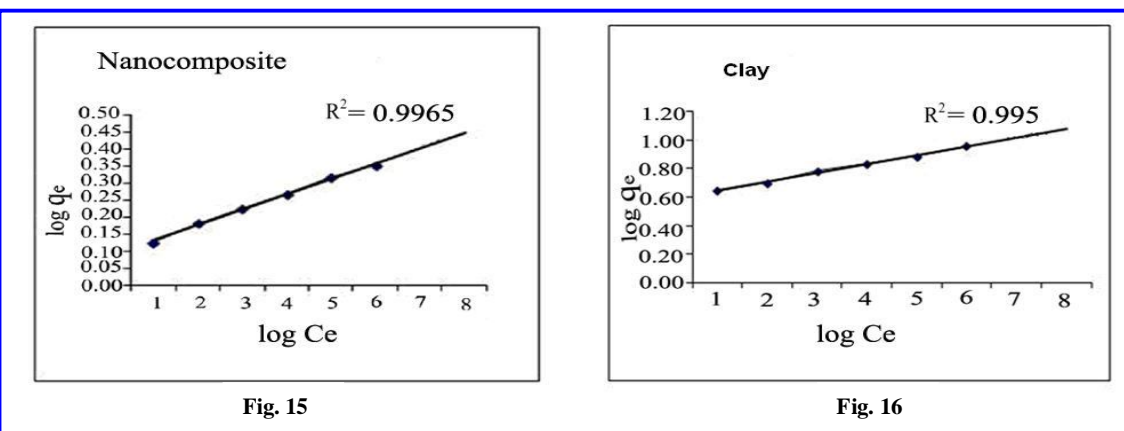


Fig. 15 & Fig. 16: Freundlich model

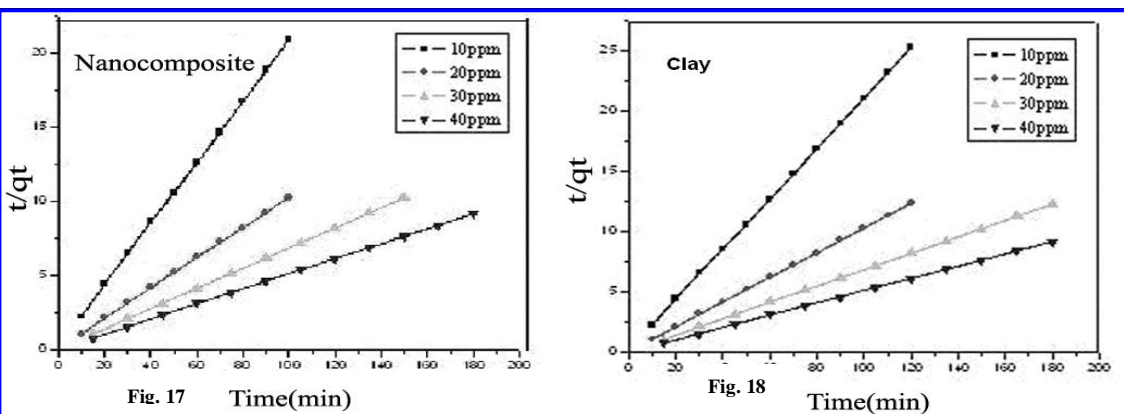


Fig. 17 & Fig. 18: Pseudo second order kinetics

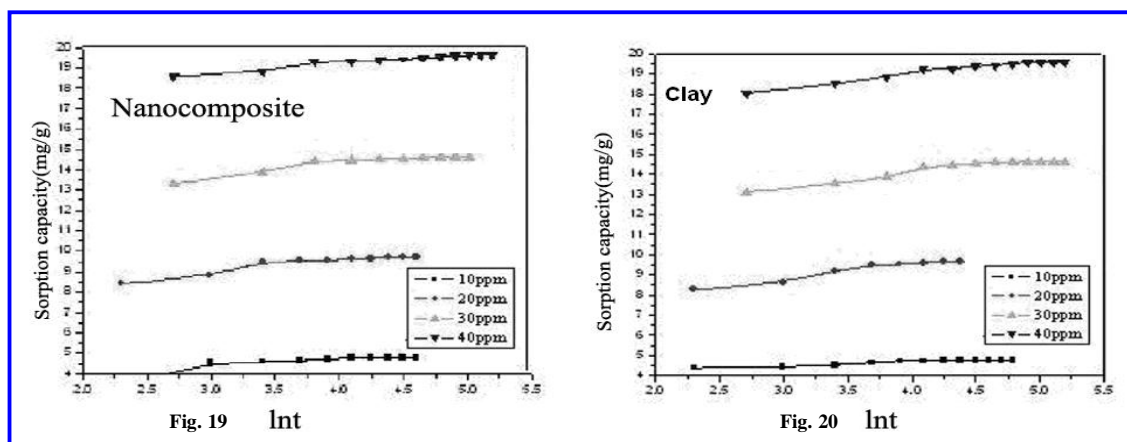


Fig. 19 & Fig. 20: Elovich kinetic model

4.3 Adsorption kinetics

In order to investigate the mechanism of adsorption of chromium by the nanocomposite and clay pseudo first order, pseudo second order and Elovich model were considered. It is observed that the data for Cr(VI) on both fire clay-TiO₂ nanocomposite and fire clay does not fit into pseudo first order kinetics.

4.4 Pseudo second order kinetics

In linearised form the pseudo second order kinetic model can be represented as

$$t/q_t = 1/k_2 q_e^2 + 1/q_e \times t \quad (4)$$

Where k_2 is the second order rate constant (g/mg min). A plot of t/q_t and 't' should be linear. q_e and k_2 can be calculated from the slope and intercept of the plot. The linear plots fig.17 & 18 obtained for the adsorption of Cr(VI) on the nanocomposite and clay at various metal ion concentrations clearly show that the adsorption process to follow pseudo second order.

4.5 Elovich kinetic model

The Elovich equation which is mainly applicable for chemisorption and often valid for systems with heterogeneous adsorbing surfaces (Karthikeyan *et al.* 2005) is generally expressed in its integrated form as

$$Q_t = (1/b) \ln(ab) + (1/b) \ln t \quad (5)$$

Where 'a' is the initial adsorption rate (mg/g min) and 'b' is related to the extent of surface coverage and the activation energy for chemisorption (g/mg). A plot of q_t vs $\ln t$ should be linear with slope $1/b$ and intercept

$\log 1/b \ln(ab)$. Fig.19 & 20 show that the plots are linear over a wide range as expected suggesting chemisorption.

4.6 Weber-Morris intraparticle diffusion model

A graphical method to prove the occurrence of intra-particle diffusion and to determine if it was the rate determining step in adsorption process was introduced by Weber and Morris (Ozcan *et al.* 2005; Weber and Morris, 1963). Intra-particle diffusion was characterized using the relationship between specific sorption (q_t) and the square root of time ($t_{1/2}$) as

$$q_t = K_{id} t_{1/2} + C \quad (6)$$

Where q_t is the amount adsorbed per unit mass of adsorbent (mg/g) at time 't' and ' K_{id} ' is the intraparticle diffusion rate constant. The linear portion of the plot for wide range of contact time between adsorbent and adsorbate does not pass through the origin suggesting that pore diffusion is the only controlling step and not the film diffusion fig. 21 & 22.

4.7 Thermodynamic parameters

The thermodynamic parameters for the adsorption process such as free energy change (ΔG°), enthalpy change (ΔH°) and entropy change (ΔS°) were evaluated using the following equations:

$$\ln K_c = \Delta S^\circ / R - \Delta H^\circ / RT \quad (7)$$

$$\Delta G^\circ = \Delta H^\circ - T\Delta S^\circ \quad (8)$$

Where K_c is the Langmuir constant related to the energy of adsorption, R is the gas constant and T is the absolute temperature (K). The values of ΔH° and ΔS° can be calculated, respectively, from the slope and intercept of the Van't Hoff plot of $\ln K_c$ versus $1/T$.

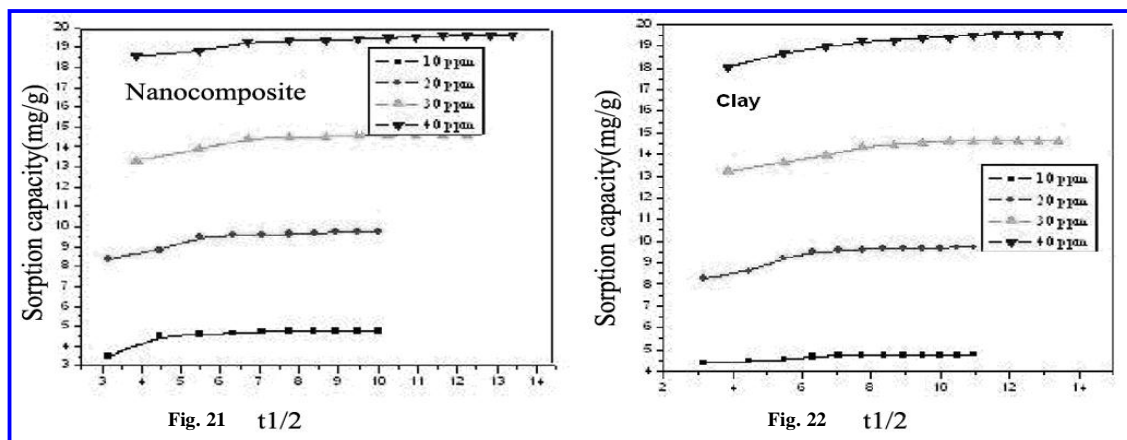


Fig. 21 & Fig. 22: Weber-Morris intraparticle diffusion model

The calculated values of ΔH° , ΔS° and ΔG° for adsorption of Cr(VI) on both nanocomposite and clay were given in table 3. Positive values of ΔH° confirms that the adsorption process to be endothermic. The negative value of ΔG° at various temperatures indicates the feasibility and spontaneity of the adsorption process. The positive value of ΔS° shows the affinity of adsorbent for Cr(VI) and it further confirms a spontaneous increase in the randomness at the solid- solution interface during the adsorption process.

Table 3: Thermodynamic parameters for adsorption of Cr (VI) on fire clay-TiO₂NC & fire clay

Adsorbent	$-\Delta G^\circ$ kJ/mol			ΔS° kJ/mol	ΔH° kJ/mol
	303K	307K	311K		
Fire clay-TiO ₂ nanocomposite	1.378	1.396	1.414	4.489	18.473
Fire clay	3.070	3.110	3.151	10.05	25.63

4.8 Desorption studies

Desorption studies with acetic acid revealed that the regeneration of adsorbent was not satisfactory, which confirms the chemisorptive nature of adsorption.

5. CONCLUSION

This study shows that the Fire clay and nanocomposite can be used effectively in the removal of Cr(VI) through adsorption. Both clay and nanocomposite followed Langmuir and Freundlich model. Pseudo second order kinetic model was followed. The sorption suggested that the adsorption is high at basic medium. Elovich kinetic model suggested that adsorption process is chemisorptive nature. The adsorption also followed by intraparticle diffusion model. The calculated values of different

thermodynamic parameters clearly indicated that the adsorption process with nanocomposite and clay was feasible, spontaneous and endothermic nature. This study also reveals showed that fire clay-TiO₂ nanocomposite exhibited higher adsorption capacity when compared to fire clay in its natural form.

REFERENCES

- Abolino, O., Aceto, M., Malandrino, M., Sarzanini, C., Mentasti, E., Adsorption of heavy metals on Na – Montmorillonite effect of p^H and Organic substances. *Water Res.*, 37, 1619-1627(2003).
- Babu, B. V. and Gupta, S., Modelling and simulation of fixed bed adsorption column effect of velocity variation, *J. Engineering & Technol.*, 1(1), 60-66(2005).
- Das, D. D., Mohapatra, R., Pradhan, J., Das, S. N. and Thakur, R. S., Adsorption of Cr(VI) from aqueous solution using activated cow dung carbon, *J. Colloid Interf. Sci.*, 232, 235–240(2000).
- Karthikeyan, G., Anitha Pius. and Alagumuthu, G., Fluoride adsorption studies of Montmorillonite clay, *Ind. J. Chem. Technol.*, 12, 263-272(2005).
- Kobya, M., Demirbas, E., Senturk, E. and Ince, M., Adsorption of heavy metal ions from aqueous solutions by activated carbon prepared from apricot stone, *Bioresources. Technol.*, 96, 1518–1521(2000).
- Langmuir, I., The constitution and fundamental properties of solids and liquids, *J. Am. Chem. Soc.*, 38, 2221-2295(1916).
- Norrozi, B., Sorial, G. A., Bahrami. H. and Arami. M., Equilibrium and kinetic adsorption study of a cationic dye by a natural adsorbent-silkworm pupa, *J. Haz. Mat.*, B, 139, 167-174(2007).
- Ozcan, A. S., Erdem, B. and Ozcan, A., Adsorption of acid blue 913 from aqueous solutions onto BTMA-bentonite, *Colloid surface A.*, 266,73-81(2005).

- Parimaladevi, D. and Venkateswaran, V., Kinetics, Thermodynamics and isothermal modelling of adsorption of triphenyl methane dyes (Methyl violet, Malachite, Magenta-2) onto fruit waste. *J. Appl. Technol. Environ. Sanitation*, 1(3), 273-283(2011).
- Pradhan, J., Das, S. N. and Thakur, R. S., Adsorption of hexavalent chromium from aqueous solution by using activated red mud. *J. ColloidInterf. Sci.*, 217, 137-141(1999)..
- Sarin, V. and Pant, K. K., Removal of chromium from industrial waste by using eucalyptus bark. *Bioresources. Technol.*, 97, 15–20(2005).
- Singh, K. K., Rastogi, R. and Hasan, S. H., Removal of Cr(VI) from wastewater using rice bran, *J. Colloid Interf. Sci.*, 290, 61–68(2005).
- Veera M. Boddu, Krishnaiah Abburi, Jonathan L. Talbott and Edgar D. Smith., *J. Environmental Science and Technol.*, Removal of hexavalent chromium from waste water using a new composite chitosan biosorbent, 37, 4449–4456(2003).
- Venkateswaran, V. and Priya, V. T., Adsorption Kinetics at thermodynamics of removal of basic dyes by fire clay, fire-TiO₂ (NC), *J. Appl. Technol. and Environ. Sanitation*, 2 (1), 7–16(2012).
- Weber, W. J., Morris, J. C., Preliminary appraisal of advanced waste treatment process, *Proc. Int. Conf., Advances in Water Poll. Res.*, 2, 231-241(1963).